Nat. Hazards Earth Syst. Sci. Discuss., 1, 3099–3127, 2013
www.nat-hazards-earth-syst-sci-discuss.net/1/3099/2013/
doi:10.5194/nhessd-1-3099-2013

Natural Hazards and Earth System Sciences
Open Access
Discussions

Wind-wave amplification mechanisms: possible models for steep wave events in finite depth

P. Montalvo[1,2], R. Kraenkel[3], M. A. Manna[1,2], and C. Kharif[4,5]

[1]Université Montpellier 2, Laboratoire Charles Coulomb UMR 5221, 34095, Montpellier, France
[2]CNRS, Laboratoire Charles Coulomb UMR 5221, 34095, Montpellier, France
[3]Instituto de Física Téorica, UNESP – Universidade Estadual Paulista, Rua Dr. Bento Teobaldo Ferraz 27, Bloco II, 01140-070, São Paulo, Brazil
[4]Ecole Centrale Marseille, 38 rue Frédéric Joliot-Curie, 13451 Marseille cedex 20, France
[5]Institut de Recherche sur les Phénomènes Hors Équilibre, CNRS, AMU, UMR 7342, 49 rue Frédéric Joliot-Curie, BP 146, 13384 Marseille cedex 13, France

Received: 10 June 2013 – Accepted: 11 June 2013 – Published: 8 July 2013

Correspondence to: M. A. Manna (miguel.manna@univ-montp2.fr)

Published by Copernicus Publications on behalf of the European Geosciences Union.

Abstract

We extend the Miles' mechanism of wind-wave generation to finite depth. A β-Miles linear growth rate depending on the depth and wind velocity is derived and allows the study of linear growth rates of surface waves from weak to moderate winds in finite depth h. The evolution of β is plotted, for several values of the dispersion parameter kh with k the wave number. For constant depths we find that no matter what the values of wind velocities are, at small enough wave age the β-Miles linear growth rates are in the known deep water limit. However winds of moderate intensities prevent the waves from growing beyond a critical wave age, which is also constrained by the water depth and is less than the wave age limit of deep water. Depending on wave age and wind velocity, the Jeffreys' and Miles' mechanisms are compared to determine which of them dominates. A wind-forced nonlinear Schrödinger equation is derived and the Akhmediev, Peregrine and Kuznetsov–Ma breather solutions for weak wind inputs in finite depth h are obtained.

1 Introduction

The pioneer theories to describe surface wind-waves growth in deep water began with the works of Jeffreys (1925); Phillips (1957) and Miles (1957, 1997) till the modern investigations that take nonlinearity and turbulence effects into account. Janssen (2004) has provided a thorough review of the topic.

1.1 Miles' and Jeffreys' mechanisms of wind wave growth

Miles' and Jeffreys' theories consider both air and water to be incompressible and disregard viscosity effects. Both theories are linear and Miles' mechanism is limited to the deep water domain. They give the linear wave growth γ_{Miles} and γ_{Jeffreys} (respectively noted γ_{M} and γ_{J}) of wind-generated normal Fourier modes of wavenumber k. In Miles theory the basic state is a shear current in air and still water. The air turbulence is disre-

NHESSD
1, 3099–3127, 2013

garded (Janssen, 2004) aside from establishing the logarithmic profile of the wind flow. The Miles mechanism of wave generation by wind states that waves are produced and amplified through a *resonance phenomenon*. Resonance appears between the wave-induced pressure gradient on the inviscid airflow and the surface waves. The resonant mechanism happens at a critical height where the airflow speed matches the phase velocity of the surface wave.

In 1925, Jeffreys produced the first plausible mechanism to explain the necessary shift of the atmospheric pressure required for an energy transfer from the wind to the waves. He assumed that this energy transfer was solely caused by a combination of form drag and flow separation. It was assumed that flow separation occurred on the leeward side of wave crests with re-attachment further down on the leeward slopes of the wave. So *flow separation* is central in Jeffrey's theory. The resulting growth rate γ_J increases with the difference between the wave phase velocity and the wind speed. Jeffreys computed γ_J for deep water (Jeffreys, 1925) and for finite depth as well (Jeffreys, 1926). Air flow separation occuring only over steep waves (Banner and Melville, 1976; Kawai, 1982), the Jeffreys' sheltering mechanism must be applied locally in time and space rather than constantly and everywhere on the wave field. Note that the sheltering mechanism is working even without proper air flow separation. In fact, there is a thickening of the boundary layer on the leeward side that generates a pressure asymmetry and consequently a sheltering effect.

1.2 The Miles' and Jeffreys' mechanisms in finite depth: basis to model freak waves events in coastal regions

Generally extreme wave events occur in the presence of wind. Kharif et al. (2008) and Touboul and Kharif (2006) investigated the influence of wind on extreme wave events using the Jeffreys' sheltering theory. They have shown that extreme events may be sustained longer by the air-flow separation. This mechanism can only be invoked if the wave is steep enough to effectively separate the air flow. Otherwise, for a too low

NHESSD
1, 3099–3127, 2013

steepness parameter ka the Jeffreys' sheltering mechanism due to flow separation becomes irrelevant.

Miles' and Jeffreys' mechanism of wind-generated surface waves in deep water was used in Touboul et al. (2008) to describe (theoretically and numerically) the evolution of a chirped wave packet under wind forcing. A comparison of the γ_M and the γ_J values corresponding to a modified Jeffreys mechanism was developed.

However, all this work is limited to deep water and hence unable to fully describe winds generating near-shore waves where the wave field is influenced by bottom bathymetry. Consequently they are not adequate to correctly describe the wind influence on extreme wave events in the coastal zone.

Therefore an extension of Miles' theory of wind-generated monochromatic waves to the case of finite depth under weak or moderate winds is needed, as well as a theoretical formulation of Jeffreys' theory in terms of adequate finite depth parameters.

The aims of this paper are: (i) to extend the Miles' mechanism to a finite depth setup, (ii) to express the Jeffreys' mechanism in terms of adequate dimensionless parameters, (iii) to determine, in terms of wave age and wind velocity, which among the Miles' and Jeffreys' mechanisms prevails and (iv) to derive a wind-forced nonlinear Schrödinger equation (NLS) in finite depth to study the effects of wind and depth on extreme wave events due to the modulational instability.

The paper is organized as follows. In Sects. 2, 2.1 and 2.2 the linear stability problem of the air–water interface is presented and the derivation of the system of equations coupling the waves to the air flow with the corresponding dispersion relation is done. In Sects. 3, 3.1 and 3.2, we write the growth rates of Miles' and Jeffreys' theories, with appropriate scalings and variables. In Sect. 4.1 the Miles' coefficient β is plotted as a function of wave age with kh constant. Next in Sect. 4.2, we present our results about the evolution of the growth rate as a function of the wave age with h constant for several wind velocities. A comparison between Miles' and Jeffreys' theory is shown and discussed in Sect. 4.3. In Sect. 5 we derive a wind-forced NLS equation in finite depth h.

NHESSD
1, 3099–3127, 2013

The Akhmediev, Peregrine and Kuznetsov–Ma breather solutions for weak wind inputs in finite depth h are exhibited. Finally in Sect. 6, conclusion and perspectives are drawn.

2 Coupling of the air and water dynamics at the interface

The fluid particles coordinates are expressed in a fixed 3-dimensional Cartesian frame Oxyz, Oz being the upwards axis. We assume the problem to be symmetric along one horizontal axis, reducing the problem to an area parallel to Oxz. We define the surface $z = 0$ as the rest state of the interface. The interface perturbation itself is denoted by η and depends on (x,t). The water depth is set at $-h$, and the air extends from the interface to infinity.

2.1 Water dynamics

The horizontal and vertical components of the fluid velocity are u and w, both depending on (x,z,t). They obey the linear Euler equations of motion in finite depth (Lighthill, 1978)

$$u_x + w_z = 0, \quad \rho_w u_t = -P_x, \quad \rho_w w_t = -P_z, \tag{1}$$

$$w(-h) = 0 \quad \text{at} \quad z = -h, \tag{2}$$

$$\eta_t = w(0) \quad \text{at} \quad z = \eta(x,t), \tag{3}$$

$$P(\eta) = P_a(\eta) + \rho_w g\eta - P_0 \quad \text{at} \quad z = \eta(x,t), \tag{4}$$

here $P = P + \rho_w gz - P_0$ is a reduced pressure with P the pressure, P_0 the total atmospheric pressure, g the gravitational acceleration and ρ_w the water density. P and P depend on (x,z,t) as well, and subscripts in u, w and P denote partial derivatives. We solve the linear equations system Eqs. (1)–(3) with

$$P = \mathcal{P}(z)e^{i\theta}, \quad u = \mathcal{U}(z)e^{i\theta},$$
$$w = \mathcal{W}(z)e^{i\theta}, \quad \eta = \eta_0 e^{i\theta}, \tag{5}$$

NHESSD
1, 3099–3127, 2013

where $\mathcal{P}$, $\mathcal{U}$ and $\mathcal{W}$ are to be found.We have the phase $\theta = k(x - ct)$ with k the wavenumber and c the phase speed. η_0 is an unknown constant. Using Eqs. (1–3) we obtain u, w and P for all (x, z, t). Then, using Eq. (4) we derive

$$\rho_w \eta_0 e^{i\theta} \{c^2 k \coth kh - g\} + P_0 = P_a(\eta). \tag{6}$$

In the archimedian interaction, $P_a(\eta) = P_0$ and Eq. (6) returns the classical phase speed expression,

$$c^2 = c_0^2 = \frac{g}{k} \tanh(kh). \tag{7}$$

We need an expression for P_a at $z = \eta$ to obtain the modified c.

2.2 Air dynamics

We examine the steady-state of a prescribed horizontal air flow, with a mean velocity U depending only on z. We denote physical quantities in the air domain by a subscript a. The air density is ρ_a, the perturbations to this steady-state are assumed to be u_a, w_a for the velocities and P_a for the pressure, all quantities depending on (x, z, t). Now, using $P_a = P_a + \rho_a\, gz - P_0$ we have

$$u_{a,x} + w_{a,z} = 0, \tag{8}$$

$$\rho_a \left[u_{a,t} + U(z) u_{a,x} + U'(z) w_a\right] = -P_{a,x}, \tag{9}$$

$$\rho_a \left[w_{a,t} + U(z) w_{a,x}\right] = -P_{a,z}, \tag{10}$$

with primes indicating differentiation with respect to z. Next we assume $P_a = \mathcal{P}_a(z) e^{i\theta}$, $u_a = \mathcal{U}_a(z) e^{i\theta}$, $w_a = \mathcal{W}_a(z) e^{i\theta}$ and we add the boundary conditions on $\mathcal{W}_a$ and $\mathcal{P}_a$,

$$\lim_{z \to +\infty} (\mathcal{W}_a' + k \mathcal{W}_a) = 0, \tag{11}$$

$$\lim_{z \to z_0} \mathcal{W}_a = W_0, \tag{12}$$

$$\lim_{z \to +\infty} \mathcal{P}_a = 0, \tag{13}$$

NHESSD
1, 3099–3127, 2013

where W_0 is a wind forcing at the surface level. The pressure and the wind perturbations are assumed to vanish at high altitudes. For the air, there is a kinematic condition as well at the aerodynamic sea surface roughness z_0, over the free surface η. In this work, z_0 will be determined by the Charnock relation (Charnock, 1955)

$$z_0 = \alpha_c \frac{u_*^2}{g}, \tag{14}$$

where u_* is the friction velocity, and assuming that $\alpha_c = 0.018$ remains constant. The kinematic boundary condition reads

$$\eta_t + U(z_0)\eta_x = w_a(z_0). \tag{15}$$

Our steady air flow $U(z)$ is set as the logarithmic wind profile

$$U(z) = U_1 \ln(z/z_0), \quad U_1 = \frac{u_*}{\kappa}, \quad \kappa \approx 0.41, \tag{16}$$

where κ is the Von Kármán constant. Such a profile is a common ground to describe wind phenomena close to the marine boundary layer (Garratt et al., 1996). Hence, we can reduce Eq. (15) to

$$\eta_t = w_a(z_0). \tag{17}$$

Then, using Eqs. (8)–(10) and (13) we obtain

$$w_a = \mathcal{W}_a e^{i\theta}, \tag{18}$$

$$u_a = \frac{i}{k}\mathcal{W}_{a,z} e^{i\theta}, \tag{19}$$

$$P_a = ik\rho_a e^{i\theta} \int_z^\infty \left[U(z') - c\right] \mathcal{W}_a(z') \mathrm{d}z'. \tag{20}$$

NHESSD
1, 3099–3127, 2013

The Rayleigh equation (Rayleigh, 1880) is then found by eliminating P_a from Eqs. (9)–(10), and is valid as long as $z > z_0$

$$(U - c)(\mathcal{W}_a'' - k^2\mathcal{W}_a) - U''\mathcal{W}_a = 0. \quad (21)$$

This equations contains a singularity at a so-called critical height z_c, where $U(z_c) = c$. All turbulence phenomena being disregarded, any possible eddies are assumed to be set below z_0, and their influence is not taken into account. We note that $\mathcal{W}_a(z)$ and c are unknown in Eqs. (18)–(21). So, we have to evaluate $P_a(\eta)$ to get c. We have then

$$P_a(\eta) = P_0 - \rho_a g\eta + ik\rho_a e^{i\theta} \int_{z_0}^{\infty} [U(z) - c]\mathcal{W}_a(z)\mathrm{d}z, \quad (22)$$

where $z = z_0$ replaces $z = \eta$ as the lower integral bound, since we are studying the linear problem. Finally, eliminating the term $ik\rho_a e^{i\theta}$ using Eq. (17), we derive

$$g(1 - s) + c\frac{sk^2}{W_0}I_1 - c^2\left\{\frac{sk^2}{W_0}I_2 + k\coth(kh)\right\} = 0, \quad (23)$$

where $s = \rho_a/\rho_w$ and $I_1 = \int_{z_0}^{\infty} U\mathcal{W}_a\,\mathrm{d}z$, $I_2 = \int_{z_0}^{\infty}\mathcal{W}_a\,\mathrm{d}z$. As the ratio density s is of order of magnitude 10^{-3}, we can develop the wave speed in Eq. (23) as $c = c_0 + sc_1 + o(s^2)$. Next, we find c_1 as a function of $\mathcal{W}_a$, which is obtained by solving Eq. (21) with $c \approx c_0$.

3 The γ_M and γ_J wind inputs

3.1 γ_M wind input

The imaginary part of c gives directly the growth rate of $\eta(x,t)$

$$\gamma_M = k\Im(c), \quad (24)$$

NHESSD
1, 3099–3127, 2013

All the physical quantities derived from the growth rate γ_M can be expressed with three parameters: δ, θ_{dw} and θ_{fd} (Young, 1997a,b)

$$\delta = \frac{gh}{U_1^2}, \quad \theta_{dw} = \frac{1}{U_1}\sqrt{\frac{g}{k}},$$
$$\theta_{fd} = \theta_{dw}\tanh^{1/2}\left(\frac{\delta}{\theta_{dw}^2}\right). \tag{25}$$

The dimensionless parameter $\delta^{1/2}$, for constant h, measures the relative value of the shallow water speed with respect to U_1. The parameter θ_{dw}, equivalent of the wave age in deep water, measures the phase speed relatively to the characteristic wind parameter U_1 in deep water, and θ_{fd} (a finite depth wave age) measures the influence of the finite depth on θ_{dw}.

In experiments, wether in wave tank or in field, the parameter C_p is used. C_p is the observed phase speed at the peak frequency Ω_p. In this paper we used in Eq. (25) the phase velocity $c = \omega/k$ of one mode instead of C_p or Ω_p. Next we choose dimensionless variables (topped by hats)

$$U = U_1\widehat{U}, \quad W_a = W_0\widehat{W}_a, \quad z = \frac{\widehat{z}}{k},$$
$$c = U_1\widehat{c}, \quad t = \frac{U_1}{g}\widehat{t}. \tag{26}$$

Using Eqs. (25) and (26) in Eq. (23) and discarding terms of order two in s we obtain c,

$$\widehat{c}(\delta,\theta_{dw}) = \theta_{dw}T^{1/2}\left(1-\frac{s}{2}\right) + \frac{s}{2}\left\{T\widehat{I}_1 - \theta_{dw}T^{3/2}\widehat{I}_2\right\}, \tag{27}$$

NHESSD
1, 3099–3127, 2013

where $T = \tanh \frac{\delta}{\theta_{dw}^2}$. With $e^{\gamma_M t}$, we obtain the dimensionless growth rate $\widehat{\gamma}_M = \frac{U_1}{g}\gamma_M$ as

$$\widehat{\gamma}_M = \frac{s}{2}\left\{\frac{T\Im(I_1)}{\theta_{dw}^2} - \frac{T^{3/2}\Im(I_2)}{\theta_{dw}}\right\}. \quad (28)$$

We have the following transformation rule between β and the dimensionless $\widehat{\gamma}_M$ (Montalvo et al., 2013)

$$\beta = \frac{2\widehat{\gamma}_M}{s}\theta_{dw}^3 T^{1/2}. \quad (29)$$

The dimensional mean energy growth rate,

$$\Gamma_M = \frac{1}{\langle E\rangle}\left\langle\frac{\partial E}{\partial t}\right\rangle, \quad (30)$$

can then be written as a function of β

$$\Gamma_M = s\beta U_1^2\left(\frac{k^3}{g}\right)^{1/2}\coth^{1/2}(kh). \quad (31)$$

3.2 γ_J wind input

Jeffreys (1926) established that the pressure component acting on a surface wave can be written as

$$P_{a,Jeffreys} = P_{a,J} = S\rho_a(U_{10} - c)^2\eta_x, \quad (32)$$

where η is the free surface elevation, S is the sheltering coefficient, always lower than unity and U_{10} is the 10 m wind velocity. This is only valid when the wave slope is larger

NHESSD
1, 3099–3127, 2013

than a certain critical value. Such a pressure gradient can also be obtained when the boundary layer thickness varies from one side of the wave crest to another, thickening on the leeward slope and resulting in a non-separated sheltering (Belcher and Hunt, 1993). We do not consider variations of the boundary layer here. Then Jeffreys assumed that the rate of work transfer from the wind to the wave is (average with respect to time)

$$\left\langle \frac{\partial E}{\partial t} \right\rangle = \left\langle P_{a,J} \cdot \left(-\frac{\partial \eta}{\partial t} \right) \right\rangle. \tag{33}$$

Our study being perturbative, we do not have any information on the possible value of η whatsoever. We assume a sinusoidal wave of the form $\eta = \eta_0 \cos k(x - ct)$, η_0 being the wave amplitude. With this, and recalling that the mean wave energy is $\langle E \rangle = \rho_w g \frac{\eta_0^2}{2}$, we can deduce the energy growth rate expression

$$\Gamma_J = \frac{k^2}{g} c s S (U_{10} - c)^2. \tag{34}$$

Now, in order to transform U_{10} in U_1, the relevant wind scale, we use the wind-stress coefficient C_{10}, as defined Wu (1982) and the Charnock relation (Charnock, 1955)

$$C_{10} = (0.8 + 0.065 U_{10}) \times 10^{-3} = \frac{u_*^2}{U_{10}^2}, \tag{35}$$

$$U_1 = \frac{U_{10}}{\kappa} \sqrt{C_{10}}. \tag{36}$$

Wu (1982) showed that the empirical Eqs. (35) and (36) proposed for light winds are even applicable in hurricane conditions. However, above a $30\,\mathrm{m\,s^{-1}}$ limit, the drag coefficient drops off the U_{10} linear progression in Eq. (35), as we can see in Fig. 1. This phenomenon reported in Powell et al. (2003) is due to the droplet saturation in a suspension layer above the sea surface. Even though it is possible to use the model developed in Makin (2004) to calculate the correct drag coefficient and friction velocity,

NHESSD
1, 3099–3127, 2013

flow separation is likely to occur at wind speeds that high, preventing Miles' mechanism from acting. Hence, we keep the range of wind speeds below this limit for computation and we can use the Eqs. (35) and (36).

4 Results

In the following Sects. 4.1, 4.2, 4.3 and 5 we present: (i) the evolution of the finite depth wind-wave input β with θ_{dw} for kh constant, (ii) its evolution, as a function of wind velocity and wave age, with h constant, (iii) a comparison between the Miles' and Jeffreys' mechanism for finite depth and a wind-forced NLS equation in finite depth.

After recalling several approximations, we are going to work with the finite depth β-Miles wind input instead of $\widehat{\gamma}_{M}$.

4.1 The finite depth β-Miles with constant kh

First, we plot in Fig. 2 the evolution of the growth rate with θ_{fd} for several constant values of the kh parameter. Neither k nor h are constants

- for large values of the theoretical wave age θ_{fd}, the values of β are in the deep water limit,
- from small to intermediate values of θ_{fd} the values of β are lower than in the deep water limit and

$$\frac{d\beta}{d\theta_{fd}} \sim 0.$$

The small values of θ_{fd} seem constrained. In fact, because all the curves are calculated with the same parameter space $h \in [0.1\,m, 18\,m]$, different bounds on kh gives different bounds on k, and subsequently on θ_{fd}. For the deep water limit $kh \approx \pi$ we rediscover Miles' result, and below the shallow water limit $kh \approx \pi/4$ we are beyond the validity of the model.

NHESSD
1, 3099–3127, 2013

4.2 The finite depth β-Miles from weak to moderate winds with h constant

In deep water, we have the classical Miles' curve $\beta(\theta_{dw})$. Herein, the introduction of the parameter δ transforms the unique curve of wave growth rate in *families of curves* $\beta(\theta_{fd})$ indexed by $\delta = gh/U_1^2$, i.e. a curve for each value of δ. Two types of families are possible:

- a family of β curves against θ_{fd} indexed by h with U_1 constant,
- a family of β curves against θ_{fd} indexed by U_1, with h constant.

The first one was studied in Montalvo et al. (2013). In this work, and for the first time, we presented curves of wave growth evolution as a function of U_1 with constant depth h. Figures 3, 4 and 5 show β curves for constant h as a function of θ_{fd}, for friction velocities U_1 from 0.5 to 2.5 m s^{-1}. More specifically, this denomination refers to a 10 m wind velocity, namely U_{10} such that

$$5 < U_{10} < 22\,\mathrm{m\,s^{-1}}.$$

One can switch from U_1 to U_{10} using simply Eq. (36). From now on, we will refer to U_{10} only. The curves show that

- no matter what the values of wind velocities are, at small enough wave age θ_{fd} the growth rate β satisfies the known deep water limit
- the consequences of finite h are visible as θ_{fd} augments. The coefficient β is lesser than in the deep water limit. Furthermore, if the finite depth wave age θ_{fd} is kept constant, the growth rate β decreases as the wind speed U_{10} augments.

Each U_{10}-curve approaches its own *theoretical* θ_{fd}*-limited growth* as β goes to zero (no energy transfer). Then, the wave propagates steadily without changing its amplitude. The θ_{fd} at which this happens is lower as the wind speed augments. Consequently, developed seas are reached faster under moderate winds than under weak winds. The

NHESSD
1, 3099–3127, 2013

evolution of β under wind intensity and wave age shown in Figs. 3, 4, and 5 is not a dynamical one, but rather a collection of wave snapshots taken at every step of the growth in height and age.

4.3 Comparison γ_M versus γ_J

Very recently, Tian and Choi (2013) investigated experimentally and numerically the evolution of deep-water waves interacting with wind, with breaking effects. They discussed the relative importance of Miles' and Jeffreys' models and showed that Miles' model may be used for waves of moderate wave steepness under weak to moderate wind forcing whereas for steep waves under strong wind forcing both mechanisms may have to be considered. In this section we desire to measure the relative importance of Miles' mechanism versus Jeffreys' mechanism in finite depth. To do that, we follow the idea in Touboul and Kharif (2006). Taking the derived growth rates from Sects. 3.1 and 3.2, one can establish the ratio between them. It reads, with only non-dimensional parameters,

$$R = \frac{\Gamma_J}{\Gamma_M} = \frac{t_M}{t_J} = \frac{ST}{\beta}\left(\frac{\kappa}{\sqrt{C_{10}}} - \theta_{fd}\right), \tag{37}$$

where $t_M = \Gamma_M^{-1}$ and $t_J = \Gamma_J^{-1}$ are the characteristic time scales of growth for the Miles and Jeffreys mechanism. Hence, we can calculate $R(U_{10}, \theta_{fd})$ to study the evolution of this ratio with the theoretical wave age, for different values of the wind speed. Each point in the (θ_{fd}, U_{10})-plane corresponds to a water depth h between 3 m and 18 m and a dispersive parameter $kh \in \left[\frac{\pi}{4}; \pi\right]$. These boundaries on kh correspond to the shallow water and deep water limits, as discussed previously. The results are shown in Fig. 6. When this ratio is significantly greater than unity, it means that the Jeffreys mechanism acts faster, and dominates. On the contrary, Miles' mechanism is dominant for values lower than unity. One can observe in finite depth that the Miles mechanism is dominant for mature waves whereas the Jeffreys mechanism is dominant for younger waves.

NHESSD
1, 3099–3127, 2013

This comparison stands as long as the wave is *steep enough* to induce a sheltering, as discussed before.

5 Wind-forced nonlinear Schrödinger equation in finite depth

Let us consider the air/water system from a *quasi-linear* point of view, i.e. the water dynamics is considered nonlinear and irrotational and, as in Miles' theory, the air flow is kept linear. So with this assumption the complete irrotational Euler equations and boundary conditions in terms of the velocity potential $\phi(x,z,t)$ are

$$\phi_{xx} + \phi_{zz} = 0 \quad \text{for} \quad -h \le z \le \eta(x,t), \tag{38}$$

$$\phi_z = 0 \quad \text{for} \quad z = -h, \tag{39}$$

$$\eta_t + \phi_x \eta_x - \phi_z = 0 \quad \text{for} \quad z = \eta(x,t), \tag{40}$$

$$\phi_t + \frac{1}{2}\phi_x^2 + \frac{1}{2}\phi_z^2 + g\eta = -\frac{1}{\rho_w} P_a \quad \text{for} \quad z = \eta(x,t). \tag{41}$$

In Miles's theory of wave generation (Miles, 1957, 1997), the complex air pressure P_a can be separated into two components, one in phase and one in quadrature with the free surface η. A phase shift between those two quantities is necessary to transfer energy from the air flow to the wave field. The transfer is only due to the part of P_a in quadrature with η. Hence, we will deal only with the acting pressure component, that is

$$P_a(x,t) = \rho_a \beta U_1^2 \eta_x(x,t), \tag{42}$$

so that the modified Bernoulli equation reads

$$\phi_t + \frac{1}{2}\phi_x^2 + \frac{1}{2}\phi_z^2 + g\eta = -s\beta U_1^2 \eta_x \quad \text{for} \quad z = \eta(x,t). \tag{43}$$

From Eqs. (38), (39), (40), and (43) we find a wind-forced finite depth NLS equation for η as a function of the standard slow space and time variables $\xi = \varepsilon(x - c_g t)$ and

NHESSD
1, 3099–3127, 2013

$v = \varepsilon^2 t$, with $\varepsilon \ll 1$ and c_g the group velocity. The perturbed NLS equation reads

$$i\eta_v + a\eta_{\xi\xi} + b|\eta|^2\eta = id\eta \tag{44}$$

with c_g, a, b and d given by Eqs. (45),(46),(47), and (48)

$$c_g = \frac{c}{2}[1 + 2kh/\sinh(2kh)], \tag{45}$$

$$a = -\frac{c_g^2 - gh[1 - khT(1 - T^2)]}{2\omega}, \tag{46}$$

$$b = \frac{k^4 c^2}{4\omega T^2}\left[\frac{9}{T^2} - 12 + 13T^2 - 2T^4 - \frac{2[2c + c_g(1 - T^2)]^2}{gh - c_g^2}\right], \tag{47}$$

$$d = s\frac{\beta}{2}\frac{U_1^2}{c^2}T\omega. \tag{48}$$

For more information about the derivation of the coefficients a and b see Thomas et al. (2012). To derive a dimensionless wind-forced NLS equation we use Eq. (26) and we obtain in the original laboratory variables x and t (after a Galilean transformation in order to eliminate the linear term $c_g\eta_x$ and dropping the hats)

$$i\eta_t + A\eta_{xx} + B|\eta|^2\eta = iD\eta \tag{49}$$

with c_g, A, B, and D now given by Eqs. (50), (51), (52) and (53)

$$c_g = \frac{1}{2\theta_{fd}}\left[1 + \frac{\delta}{\theta_{dw}^2}\frac{1 - T^2}{T}\right], \tag{50}$$

NHESSD
1, 3099–3127, 2013

$$A = -\frac{c_g^2 - \delta\left[1 - \delta\theta_{dw}^{-2}(1 - T^2)\right]}{2\theta_{fd}\theta_{dw}^2}, \tag{51}$$

$$B = \frac{1}{4T^2\theta_{fd}^3\theta_{dw}^2}\left[\frac{9}{T^2} - 12 + 13T^2 - 2T^4 - \frac{2\left[2\theta_{fd}^{-1} + c_g(1 - T^2)\right]^2}{\delta - c_g^2}\right], \tag{52}$$

$$D = s\frac{\beta}{2}\frac{T^{1/2}}{\theta_{dw}^3}. \tag{53}$$

Equation (49) is a wind-forced finite depth NLS equation in dimensionless variables.

5.1 The Akhmediev, Peregrine and Ma solutions for weak wind inputs in finite depth

The classical nonlinear Schrödinger equation provides a model for *freak waves*, see for example Touboul and Kharif (2006); Touboul et al. (2008); Kharif et al. (2008) and references therein. The wind-forced nonlinear Schrödinger equation allows the study of the wind influence on the freak waves dynamics (Touboul and Kharif, 2006; Touboul et al., 2008; Kharif et al., 2008; Onorato and Proment, 2012). Previous authors have carried out such studies in deep water. The present work allows, for the first time, similar studies in finite depth with the right Miles' growth rates.

In the following we are going only to consider the so called focusing NLS equation, i.e. positives A and B. Introducing η' and x' as

$$\eta' = \sqrt{B}\eta, \quad x' = \frac{x}{\sqrt{A}},$$

NHESSD
1, 3099–3127, 2013

Equation (49) transforms, dropping the primes, into

$$i\eta_t + \eta_{xx} + |\eta|^2\eta = iD\eta. \tag{54}$$

Introducing a function $M(x,t)$ as

$$M(x,t) = \eta(x,t)\exp(-Dt), \tag{55}$$

we obtain from Eq. (54)

$$iM_t + M_{xx} + \exp(2Dt)|M|^2M = 0. \tag{56}$$

In order to reduce Eq. (54) into the standard form of the NLS with constant coefficients we proceed in the following way. First of all we consider the wind forcing $2Dt$ to be weak, such that the exponential can be approximated by $\exp(-2Dt) \sim 1 - 2Dt$ so we have

$$iM_t + M_{xx} + n|M|^2M = 0, \quad n = n(t) = 1 - 2Dt. \tag{57}$$

Now with a change of coordinates from (x,t) to (z,τ) defined by

$$z(x,t) = xn(t), \quad \tau(x,t) = xn(t), \tag{58}$$

and scaling the wave envelope as (Onorato and Proment, 2012)

$$M(z,\tau) = \Psi(z,\tau)\sqrt{n(\tau)}\exp\left(\frac{-iDz^2}{n(\tau)}\right), \tag{59}$$

we reduce Eq. (57) to the standard focusing equation for $\Psi(z,\tau)$

$$i\Psi_\tau + \Psi_{xx} + |\Psi|^2\Psi = 0. \tag{60}$$

NHESSD
1, 3099–3127, 2013

Equation (60) admits well known breather solutions that are simple analytical prototypes for rogue wave events. They are the Akhmediev (Ψ_A) (Akhmediev et al., 1987), the Peregrine (Ψ_P) (Peregrine, 1983) and the Kuznetsov–Ma (Ψ_M) (Ma, 1979) breather solutions.

Dysthe and Trulsen (1999) investigated whether freak waves in deep water could be modeled by Ψ_A, Ψ_P or by Ψ_M. Onorato and Proment (2012) considered the influence of weak wind forcing and dissipation on these Ψ_A, Ψ_P or Ψ_M solutions in deep water.

The present work allows us to go ahead and to exhibit expressions for Ψ_A, Ψ_P and Ψ_M *under the influence of weak wind forcing in finite depth h given by the extended Miles mechanism.* These solutions read (Dysthe and Trulsen, 1999):

$$\eta_A = P(\tau)\left\{\frac{\cosh(\Omega\tau - 2i\omega) - \cos(\omega)\cos(pz)}{\cosh(\Omega\tau) - \cos(\omega)\cos(pz)}\right\}, \tag{61}$$

with $p = 2\sin(\omega)$, $\Omega = 2\sin(2\omega)$ ω real and p related to the spatial period $2\pi/p$

$$\eta_P = P(\tau)\left\{1 - \frac{4(1+4i\tau)}{1+4z^2+16\tau^2}\right\}, \tag{62}$$

$$\eta_M = P(\tau)\left\{\frac{\cos(\Omega\tau - 2i\omega) - \cosh(\omega)\cosh(pz)}{\cosh(\Omega\tau) - \cos(\omega)\cos(pz)}\right\}, \tag{63}$$

with $p = 2\sinh(\omega)$, $\Omega = 2\sinh(2\omega)$ and Ω real and related to the time period $2\pi/\Omega$ and

$$P(\tau) = n(\tau)\exp\left[\frac{-iDz^2}{n(\tau)}\right]\exp[2i\tau].$$

A more detailed analytical and numerical analysis in terms of x and t of Eq. (49) will be developed in a future work.

NHESSD
1, 3099–3127, 2013

6 Conclusions

We have extended the well known Miles' theory to the finite depth case under breeze to moderate wind conditions. We have linearized the equations of motion governing the dynamics of the air/water interface problem in finite depth and we have investigated the linear instability in time of a normal Fourier mode of wave-number k in Miles' and Jeffreys mechanisms in finite depth. For the Miles' mechanism we have shown that normal modes are unstable and grow exponentially in time as

$$\exp\left[\frac{s\beta}{2\theta_{\mathrm{fd}}^{3}T^{1/2}}\right]t.$$

with β the finite depth Miles' coefficient. The curves of β against θ_{fd} with kh constant showed essentially that the values of β remain smaller than those corresponding to the deep water limit $\forall\theta_{\mathrm{fd}}$. Wind effects on the temporal growth have been discussed. From a comparison between the growth rates γ_{M} and γ_{J} a diagram in the $(\theta_{\mathrm{fd}},U_{10})$ plane displays the domains where the Miles' mechanism ($R < 1$) or the Jeffreys' mechanism ($R > 1$) is dominant.

We have derived for the first time a wind-forced finite depth nonlinear Schrödinger equation. The wind forcing is based on the Miles' theory extended to finite depth. This equation admits the Akhmediev, Peregrine and Kuznetsov–Ma breather solutions for weak wind input in finite depth.

Many parameters influence the mechanisms of wave growth under wind action, in finite depth. For instance time variations of wind speed and wind direction, the bathymetry effects in the field, loss of energy by bottom friction, air flow-induced surface drifts, turbulence, nonlinear interactions between waves, flow separation, dissipation due to white capping and so on. The scope of this paper is not to address all of these phenomena.

NHESSD
1, 3099–3127, 2013

Nevertheless, we believe that this work could be useful for the understanding of wave generation in finite-depth situations, namely in the coastal zone. The present theory is the first step towards more accurate freak waves models in finite depth.

Acknowledgements. P. M. thanks *Labex NUMEV* (Digital and Hardware Solutions, Modeling for the Environment and Life Sciences) for partial financial support.

M.A.M thanks *PVE program* (Pesquisador Visitante Especial, CAPES/BRASIL) for financial support.

References

Akhmediev, N. N., Eleonskii, V. M., and Kulagin, N. E.: Exact first-order solution on the nonlinear Schrödinger equation, Theor. Math. Phys., 72, 809–818, 1987. 3117

Banner, M. and Melville, W.: On the separation of air flow over water waves, J. Fluid Mech., 77, 825–842, 1976. 3101

Belcher, S. E. and Hunt, J. C. R.: Turbulent shear flow over slowly moving waves, J. Fluid Mech., 251, 109–148., 1993. 3109

Charnock, H.: Wind stress on a water surface, Q. J. Roy. Meteor. Soc., 81, 639–640, 1955. 3105, 3109

Dysthe, K. B. and Trulsen, K.: Note on Breather Type Solutions of the NLS as Models for Freak-Waves, Phys. Scripta, T82, 48–52, 1999. 3117

Garratt, J., Hess, G., Physick, W., and Bougeault, P.: The atmospheric boundary layer advances in knowledge and application, Bound.-Lay. Meteorol., 78, 9–37, 1996. 3105

Janssen, P.: The Interaction of Ocean Waves and Wind, Cambridge University Press, UK, 2004 2004. 3100, 3101

Jeffreys, H.: On the formation of water waves by wind, P. R. Soc. Lond. A-Conta., 107, 189–206, 1925. 3100, 3101

Jeffreys, H.: On the formation of water waves by wind (Second paper), P. R. Soc. Lond. A-Conta., 110, 241–247, 1926. 3101, 3108

Kawai, S.: Structure of air flow separation over wind wave crests, Bound.-Lay. Meteorol., 23, 503–521, 1982. 3101

NHESSD

1, 3099–3127, 2013

Kharif, C., Giovanangeli, J.-P., Touboul., C., Grade, L., and Pelinovsky, E.: Influence of wind on extreme wave events: experimental and numerical approaches, J. Fluid Mech., 594, 209–247, 2008. 3101, 3115
Lighthill, J.: Waves in Fluids, Cambridge University Press, UK, 1978. 3103
Ma, Y.: The perturbed plane-wave solutions of the cubic Schrödinger equation, Stud. Appl. Math, 60, 43–58, 1979. 3117
Makin, V.: A note on the drag of the sea surface at hurricane winds, Bound.-Lay. Meteorol., 115, 169–176, 2004. 3109
Miles, J.: On the generation of surface waves by shear flows, J. Fluid Mech., 3, 185–204, 1957. 3100, 3113
Miles, J.: Generation of surface waves by winds, Appl. Mech. Rev, 50-7, R5–R9, 1997. 3100, 3113
Montalvo, P., Dorignac, J., Manna, M., Kharif, C., and Branger, H.: Growth of surface wind-waves in water of finite depth, a theoretical approach, Coast. Eng., 77, 49–56, doi:10.1016/j.coastaleng.2013.02.008, 2013. 3108, 3111
Onorato, M. and Proment, D.: Approximate rogue wave solutions of the forced and damped Nonlinear Schrödinger Equation for water waves, Phys. Lett. A, 376, 3057–3059, 2012. 3115, 3116, 3117
Peregrine, D.: Water waves, nonlinear Schrödinger equation and their solutions, J. Austral. Math. Soc. Ser. B, 25, 16–43, 1983. 3117
Phillips, O.: On the generation of waves by turbulent wind, J. Fluid Mech., 2, 417–445, 1957. 3100
Powell, M., Vickery, P., and Reinhold, T.: Reduced drag coefficient for high speeds in tropical cyclones, Nature, 422, 279–283, 2003. 3109
Rayleigh, L.: On the stability or instability of certain fluid motions, P. Lond. Math. Soc., 11, 57–70, 1880. 3106
Thomas, R., Kharif, C., and Manna, M. A.: A nonlinear Schrödinger equation for waves on finite depth with constant vorticity, Phys. Fluids, 24, 138–149, doi:10.1063/1.4768530, 2012. 3114
Tian, Z. and Choi, W.: Evolution of deep-water waves under wind forcing and wave breaking effects: numerical simulations and experimental assessment, Eur. J. Mech. B-Fluid., 41, 11–22, doi:10.1016/j.euromechflu.2013.04.001, 2013. 3112

NHESSD
1, 3099–3127, 2013

Touboul, J. and Kharif, C.: On the interaction of wind and extreme gravity waves due to modulational instability, Phys. Fluids, 18, 108103-1–108103-4, doi:10.063/1.2374845, 2006. 3101, 3112, 3115

Touboul, J., Kharif, C., Pelinovsky, E., and Giovanangeli, J.-P.: On the interaction of wind and steep gravity wave groups using Miles' and Jeffreys' mechanisms, Nonlin. Processes Geophys., 15, 1023–1031, doi:10.5194/npg-15-1023-2008, 2008. 3102, 3115

Wu, J.: Wind-stress coefficients over sea surface from breeze to hurricane, J. Geophys. Res., 87, 9704–9706, 1982. 3109

Young, I.: The growth rate of finite depth wind-generated waves, Coastal Eng., 32, 181–195, 1997a. 3107

Young, I.: Wind Generated Ocean WWaves, Elsevier, Kidlington, Oxford, UK, 1997b. 3107

NHESSD

1, 3099–3127, 2013

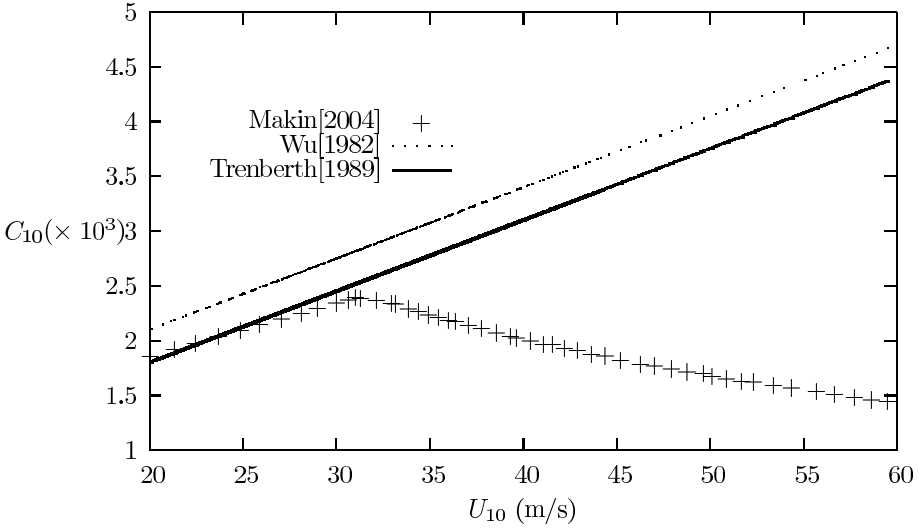

Fig. 1. The drag coefficient versus the U_{10} wind velocity. As we can see, it follows a linear progression until its maximum around 30 m s^{-1}, then decreases. So, a linear parametrization of C_{10} is a reasonable approximation.

NHESSD
1, 3099–3127, 2013

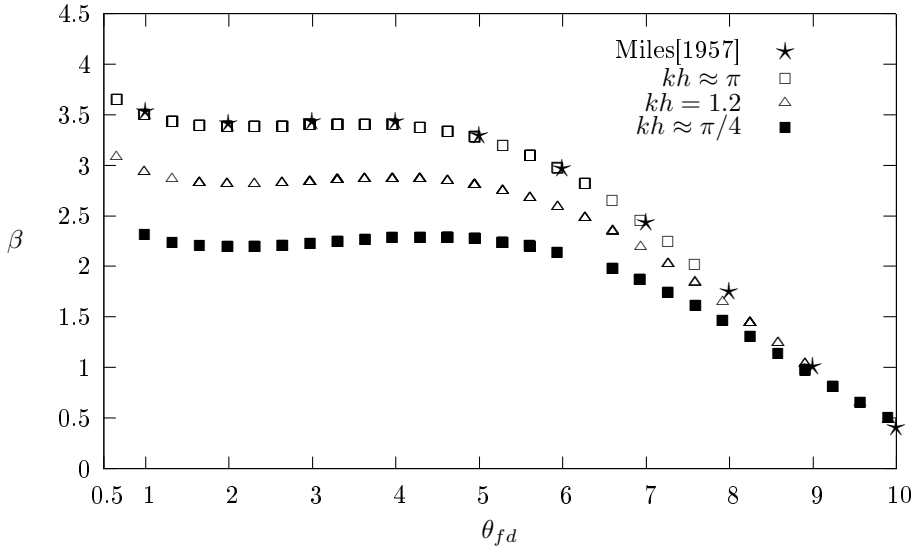

Fig. 2. Miles'β vs θ_{fd}. For the deep water limit $kh \approx \pi$ our results fit the Miles' curve. $kh < \pi/4$ corresponds to shallow water that is beyond the range of validity of our model. An intermediate value of kh is included, and we see that β is less than in the deep water limit.

NHESSD
1, 3099–3127, 2013

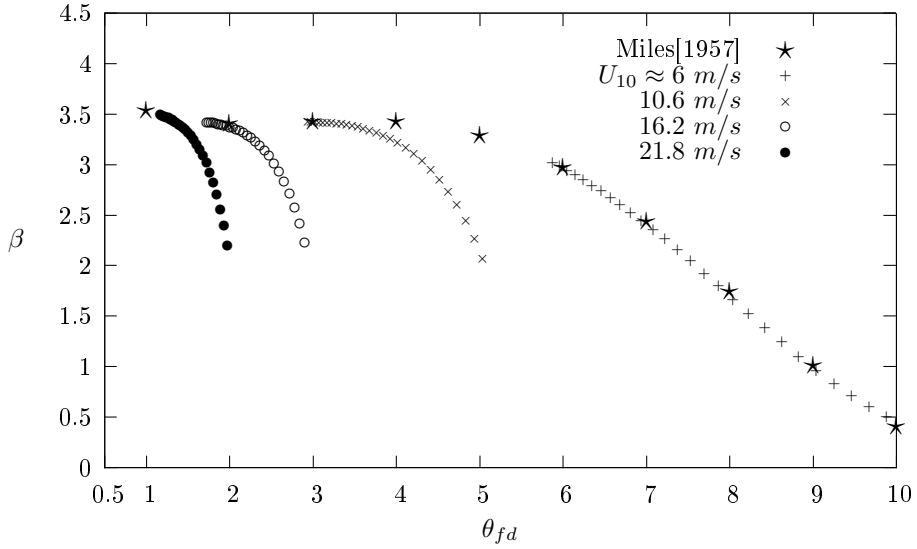

Fig. 3. β vs. θ_{fd}, the wage-age like parameter. The water depth is $h = 3$ m for all curves above. For this depth, all 10 m wind speeds account for early drops in the growth rate. The deep water limit $kh \to \infty$, originally computed by Miles, is plotted for comparison. For the lower wind speed, the growth drop occurs closer to deep water. Although $U_{10} = 6\,\mathrm{m\,s^{-1}}$ gives a deep water-like behaviour, we see that stronger winds implies early (wavelength-wise) drops in the growth rate.

NHESSD
1, 3099–3127, 2013

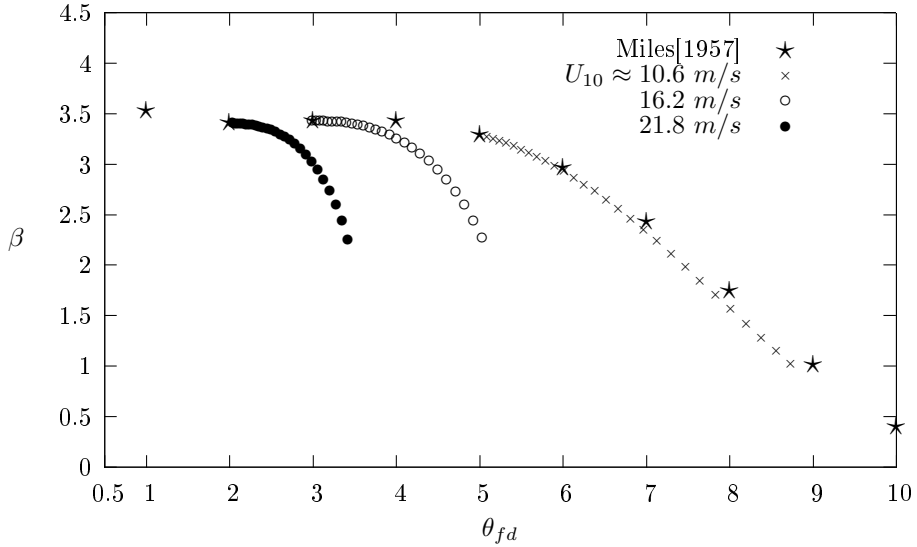

Fig. 4. Same as Fig. 3 with $h = 9$ m. The lowest wind speed $U_{10} \approx 6.0\,\mathrm{m\,s^{-1}}$ is not shown, as the next one already gives us a deep water limit.

NHESSD
1, 3099–3127, 2013

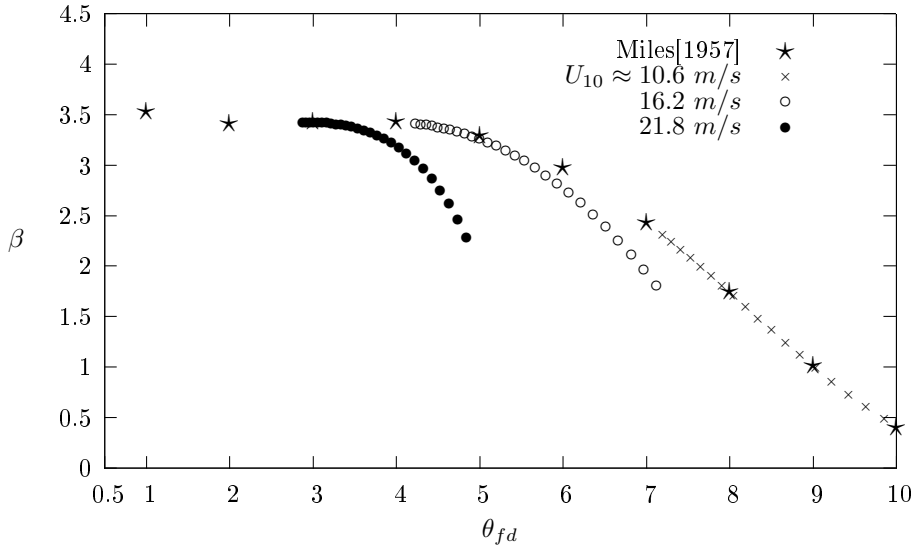

Fig. 5. Same as Fig. 4 with h = 18 m.

NHESSD
1, 3099–3127, 2013

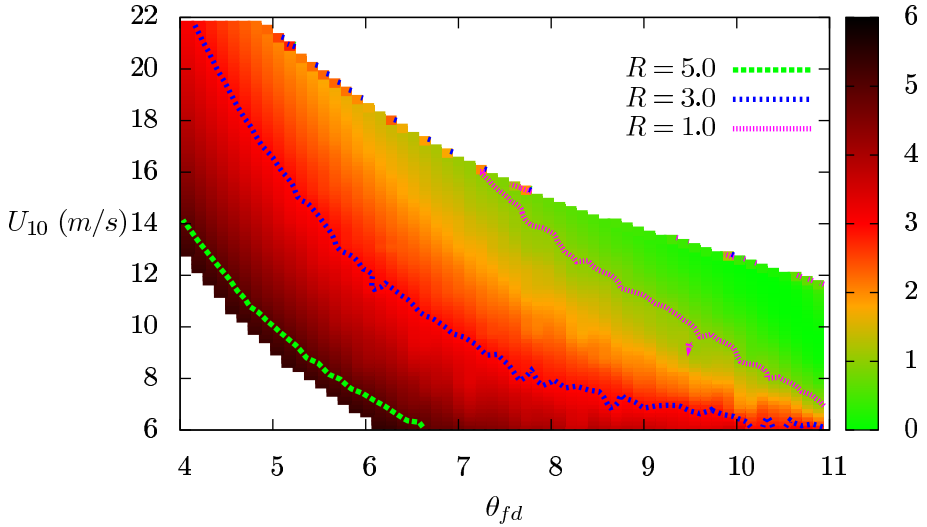

Fig. 6. (U_{10}, θ_{fd})-parameter space for continuously varying values of $R = \Gamma_J/\Gamma_M$. In the domain defined by $R < 1$, the Miles' mechanism is dominant whereas for $R > 1$, the Jeffreys' mechanism is dominant.

NHESSD
1, 3099–3127, 2013